Sintering and conductivity of nano-sized 8 mol% YSZ synthesized by a supercritical CO_2-assisted sol-gel process

M. Klotz[1*], D. Marinha[1], C. Guizard[1], A. Addad[2], A. Hertz[3], F. Charton[3]

[1] Laboratoire de Synthèse et Fonctionnalisation des Céramiques, UMR 3080 Saint-Gobain CREE/CNRS, 550 Avenue Alphonse Jauffret, 84306 Cavaillon, France, michaela.klotz@saint-gobain.com
[2] UMET - Unité Matériaux et Transformations, Université Lille1 Bâtiment C6, 59655 Villeneuve d'Ascq, France
[3] Laboratoire des Procédés Supercritiques et de Décontamination; CEA Marcoule - DEN/DTCD/SPDE/LFSM ; BP17171 - 30207 Bagnols sur Cèze - France

INTRODUCTION

The possibility to synthesize nano-sized powders has particular advantages for specific practical applications. The strong thermal reactivity of fine powders is key in obtaining dense ceramic bodies with small grain size. These types of microstructures present known advantages for mechanical properties, but may also increase oxygen mobility in both ionic and mixed ionic and electronic conductors [1,2]. However, to obtain high densification rates and small grain size (< 100 nm), careful control of the sintering conditions is required. In particular, grain-boundary interfaces dominate electric behavior and residual, porosity may be extremely difficult to avoid and/or eliminate. Ceramic 8/YSZ (8 mol% yttria stabilized zirconia) is a very reliable ion conducting material widely used as electrolyte in solid oxide fuel cells, functioning above 900 °C. Significant effort is consistently being made to increase 8/YSZ conductivity at lower temperatures in order to decrease materials requirements and increase overall lifetime so to decrease the operation costs.
Among available synthesis techniques for ceramic powders with high specific surface area, supercritical fluids-based methods are of particular interest. They combine medium synthesis temperature avoiding grain growth and supercritical drying preventing particles aggregation. The aim of the present study is to evaluate the potential of 8/YSZ powder, synthesized under supercritical conditions.

SYNTHESIS AND CHARACTERIZATION

In this work, nano-metric 8/YSZ powder was synthesized using a supercritical carbon dioxide aided sol-gel process developed at the CEA/LPSD. Detailed synthesis conditions and characterizations are reported in [3]. Crystallites are typically smaller than 10 nm (*Figure 1*), leading to a very high specific surface area of 170 $m^2.g^{-1}$. TEM images clearly display the crystalline nature of the nanoparticles. It should be noted that two types of aggregation states are systematically found, where a rather dispersed state coexists with a more compact state. The aggregation state has been shown to be governed by synthesis parameters [3].

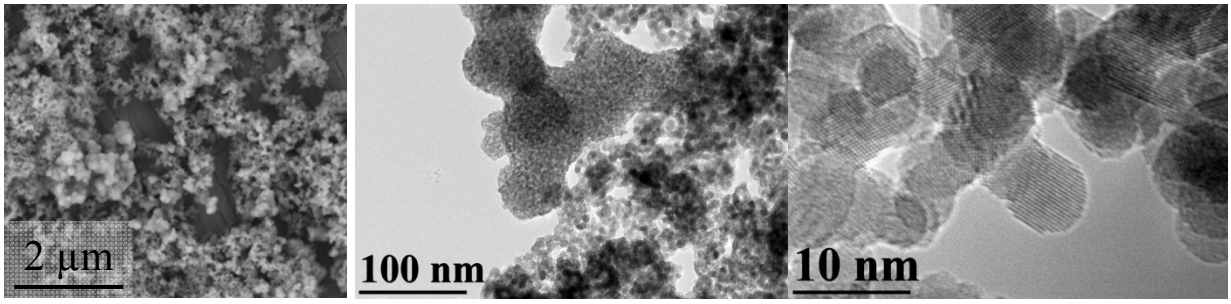

(a) (b) (c)

Figure 1: (a) SEM and (b,c) TEM images 8/YSZ powder used.

Powders were densified using Spark Plasma Sintering (SPS) to avoid grain growth during sintering. 2.5 g of powder were placed into 20 mm diameter graphite molds. Maximum temperature was varied between 1000 °C and 1200 °C with a constant dwell time of 15 minutes. Uniaxial pressure of 76 MPa was applied over the whole cycle. All trials were performed under vacuum.

In a first attempt, the powders were used as-recovered from the CO_2-assisted synthesis. However, sintering resulted in breaking of the samples into dark black fragments. Post-mortem analysis showed graphite inclusions, due to 6.8 % of residual organics in the powder. In order to remove the residual organic, a pretreatment at 500 °C for 1 h (heating rate 140 °C/h) was performed prior to sintering. This decreased the specific surface area from 170 $m^2.g^{-1}$ to 140 $m^2.g^{-1}$. This method was efficient and proper sintered samples were obtained. The relative density was determined either geometrically or by Archimedes considering a theoretical density of 8/YSZ of 5.90 $g.cm^{-3}$. The geometrical density is systematically lower than using Archimedes, indicating probable enclosed porosity. XRD analysis, displayed in the 25-40°-2θ range, of the sintered samples (Figure 2) showed fully-stabilized pure cubic phase, as expected for 8/YSZ.

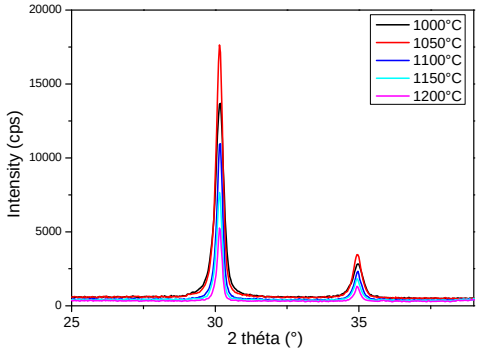

Figure 2: XRD of sintered samples.

Sintering Temperature (°C)	Relative density (%)	
	Geometric	Archimedes
1000	61 %	67 %
1050	85 %	86 %
1100	91 %	95 %
1150	97 %	97 %
1200	95 %	99 %

Table 1: Relative densities of sintered samples.

The samples were further studied by TEM on thin foils. For each sintering temperature, microstructures are composed of well-densified domains co-existing with nano-sized porosity domains. Figure 3 shows the interface between two such domains. The grain growth as a function of the density of the sample was determined separately for each domain. As reported on Figure 4, the porous domains are much more resistant to sintering. The dense domains

react similarly to the behavior of commercial 3/YSZ powder [4]. Neither inter-granular porosities nor an amorphous film at the grain boundary could be evidenced by TEM on the dense zone, as shown on Figure 5 for the 1150 °C sintered sample.

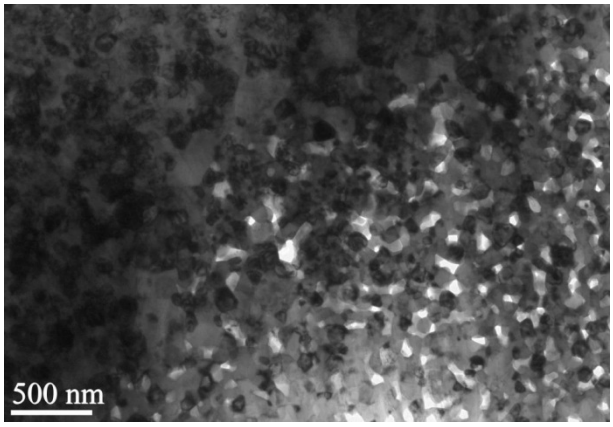

Figure 3: TEM – Coexistence of dense and porous domains (sintered at 1150°C).

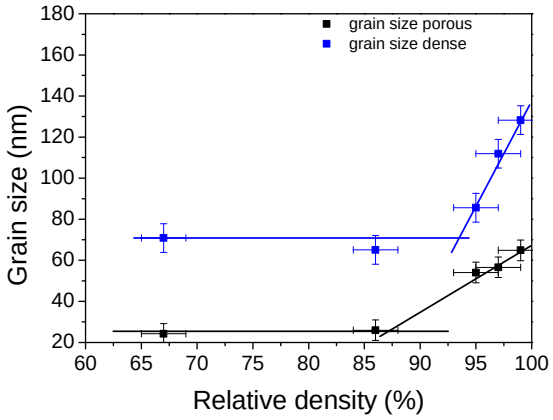

Figure 4: Sintering curves: grain growth of dense and porous domains as a function of sample density.

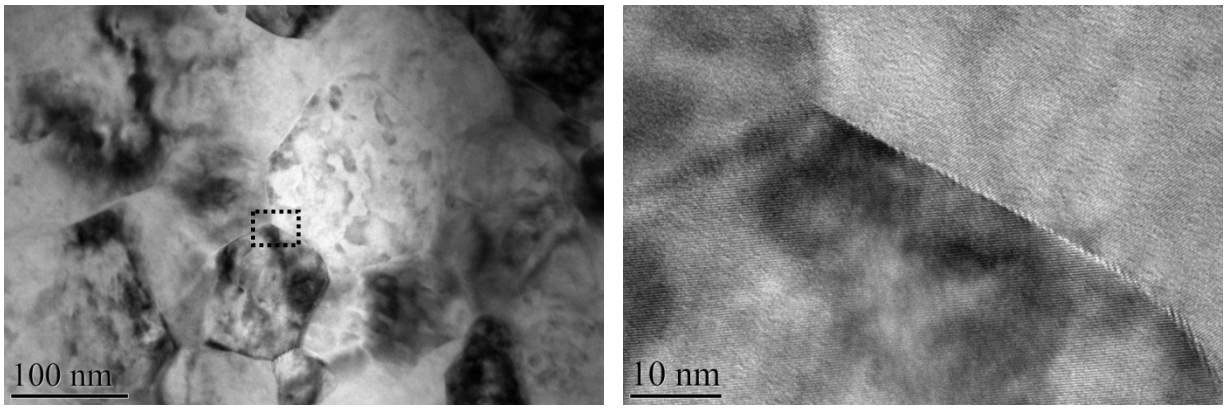

(a) (b)

Figure 5 : Dense zone, sample sintered at 1150 °C (a), grain boundary detail (b).

CONDUCTIVITY

Methodology

Platinum paste was used to paint the electrodes on both planar surfaces of the pellets and annealed at 800 °C for 2h. Impedance measurements were performed in two-electrode configuration between 200 and 800 °C at 50 °C intervals with 1.5 h for temperature stabilization. Signal frequency was limited between 37 MHz and 1 Hz with amplitude of 100 mV.

Impedance Spectroscopy results

Typical polycrystalline YSZ impedance spectra displays two arcs in the Z' vs Z'' plane, also known as Nyquist plot. The high frequency arc corresponds to bulk while the low frequency one corresponds instead to the grain boundary. An additional arc appears at even lower frequencies, corresponding to the electrode response. In this case, an equivalent electrical circuit composed of two RC* elements in series is used to fit the experimental response and extract relevant parameters of associated resistance, frequency and capacitance for each response for each contribution. In contrast, spectra for the samples in this study are composed of one complete and an incomplete arcs at high and low frequencies, respectively. At higher measuring temperatures the low frequency response is better defined.

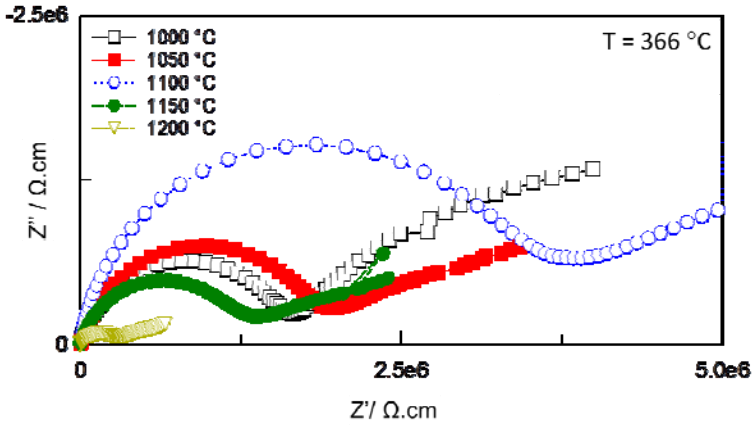

Figure 6: Comparison of normalized impedance spectra collected at 366 °C for all samples.

At this moment, one can only speculate as to the exact reasons for this effect. The response frequency, $f = 1/2\pi RC$, where R is resistance and C the capacitance, both of which are calculated by fitting of experimental data. Consequently, the response frequency is equally affected by both capacitance as well as resistance.

Nevertheless, this effect has not been observed in similarly processed 3YSZ obtained by SPS [5] Fitting of the full spectra was made using two R//CPE elements (Figure 7), in order to account for the depressed arc as well.

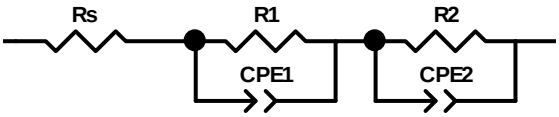

Figure 7: Equivalent circuit used for fitting of the spectra.

Fitting quality was often below standard, especially at low temperatures, where the convoluted arc was not properly fitted.

The total conductivity (inverse sum of both detected contributions) plots do not show an explicit trend in across samples, although the values are roughly an order of magnitude below those of typical polycrystalline 8/YSZ.

* In practice, because the capacitive response is not homogeneous, a constant phase element, *CPE*, is used to replace the capacitor.

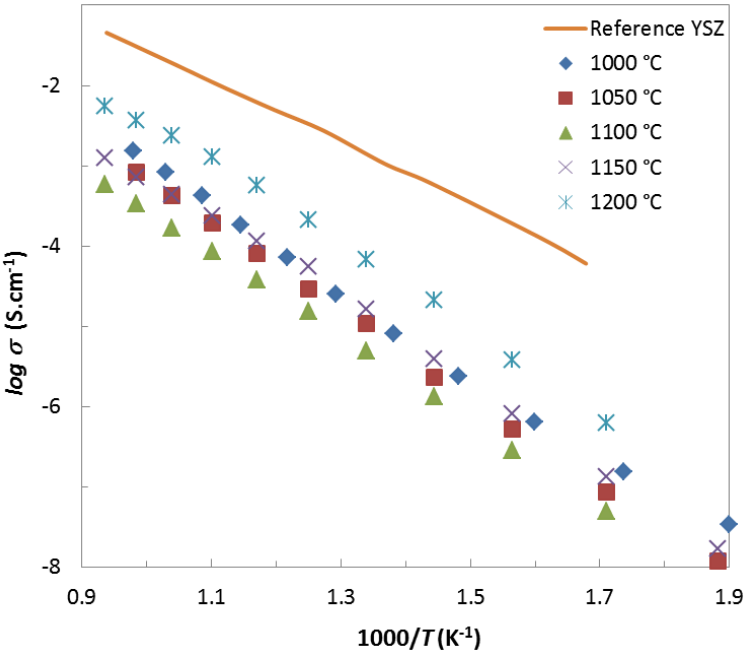

Figure 8: Conductivity plots for all samples (symbols) compared with reference values for 8YSZ (line) from [6].

Data were corrected for porosity using Equation 1, where σ refers to conductivity ($S.cm^{-1}$) and ρ to relative density. This allows estimating the total conductivity for an ideally dense sample. There are no major differences when plotting data corrected for porosity (Figure 9), as samples sintered at 1100 °C and above have relative densities close to unit. On the other hand, sample sintered at 1000 °C displays an increase which places it near the maximum conductivity value obtained by sample sintered at 1200 °C.

$$\sigma_{porous} = \sigma_{dense} \times \rho_r^{2.5} \qquad \text{Equation 1}$$

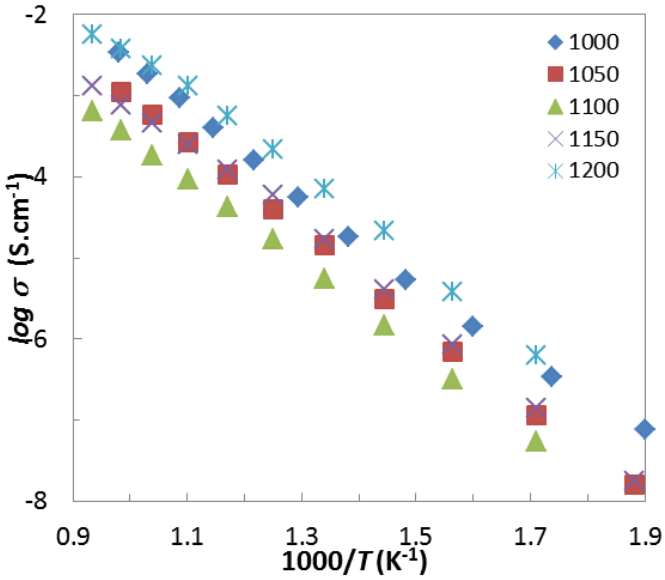

Figure 9 – Total sample conductivity corrected for sample porosity.

The characteristic frequency of the convoluted arc is plotted against temperature and values are found to be coherent across samples, although with some changes in slope which reflect the relative poor quality of the fits.

The capacitance values associated with the high-frequency response were determined to be of the order of 10^{-12} F, which is typical of the bulk response (Figure 10). The capacitance values associated with the second arc at low frequencies were determined to be of the order of 10^{-9} F, which is typical of grain boundaries. This discards the possibility of being due to the platinum electrodes, which instead should be of the order of 10^{-4} F. This interpretation implies that the associated resistance is large and heterogeneous across samples. Given that the TEM imaging shows clean grain boundaries, one can fairly assume that the additional resistance is in fact due to the nanometric sized pores that populate the microstructure.

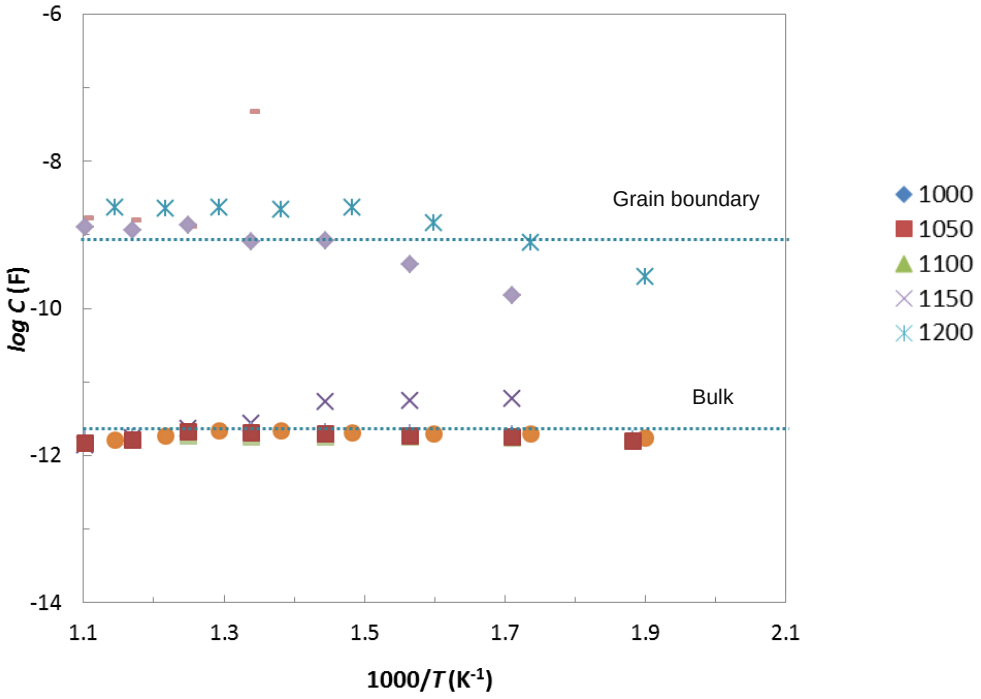

Figure 10 : High-frequency (bulk) and low-frequency (grain boundary) capacitance values as a function of temperature. Dotted lines were added only as visual guide lines.

Conductivity values obtained for the best sample in this work (1200°C), were compared with published results. At 600°C the conductivity found for this sample (7.8×10^{-4} S.cm^{-1}) is about one order of magnitude lower than the conventionally prepared sample: 7.6×10^{-3} S.cm^{-1}.

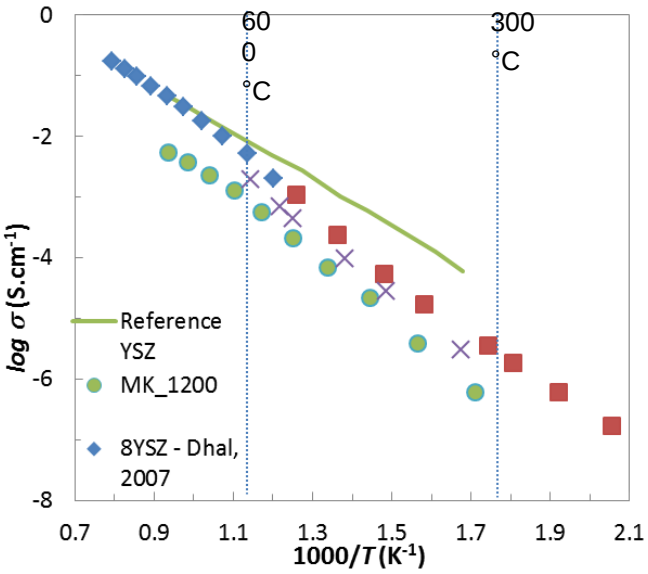

Figure 11 – Comparison of conductivity data for 1200°C sample and literature results.

CONCLUSION

The sintering and conductivity of 8/YSZ nano-powder, synthesized using a supercritical CO_2 assisted sol-gel process, was investigated. This work showed that the residual organic of the as-synthesized nanopowder prevents proper sintering. The residual organic was eliminated by thermal pre-treatment at 500°C. Sintered samples with maximum relative densities of 95 % were obtained and TEM observation showed grain size varying between 60 and 120 nm within the same sample. TEM further showed that the grain boundaries are clear of defects although residual closed porosity is heterogeneously present. Conductivity measurements were performed by impedance spectroscopy in air between 200 and 800 °C. The resulting spectra display a single electric response, which is not unusual in nano-sized microstructures and may be explained by convolution of grain-boundary and bulk response frequencies due to nano-metric grain size. The best sample has conductivity of 7.8×10^{-4} S.cm^{-1} at 600 °C. This however is one order of magnitude lower than for samples prepared using conventional powders. This result is linked to the heterogeneous residual porosity. Improvement of the microstructure could be obtained by using more homogeneous powder, thus by improving the pre-aggregation of the powder. More particularly, the thermal pre-treatment used to eliminate the residual organic content is thought to lead to an initial sintering that is difficult to destroy during the spark plasma sintering. Other methods of organic removal should therefore be investigated to fully assess the potential of this nano-sized 8/YSZ powder as a conductive ceramic.

Acknowledgments:

Guillaume Bonnefont from Insa Lyon is acknowledged for help with the SPS sintering. The TEM facility in Lille (France) is supported by the Conseil Regional du Nord-Pas de Calais, and the European Regional Development Fund (ERDF).

REFERENCES

[1] O. J. DURA, M. A. L. DE LA TORRE, L. VAZQUEZ, J. CHABOY, R. BOADA, A. RIVERA-CALZADA, J. SANTAMARIA, C. LEON; Phys. Rev. B, vol. 81, no. 18, **2010,** p. 1
[2] J. RUPP and L. GAUCKLER, Solid State Ionics, vol. 177, no. 26–32, **2006**, p. 2513
[3] A. HERTZ, M. DROBEK, J.-C. RUIZ, S. SARRADE, C. GUIZARD, A. JULBE, Chemical Engineering Journal, vol. 228, **2013,** 622
[4] G. BERNARD –GRANGER, A. ADDAD, G. FANTOZZI, G. BONNEFONT, C. GUIZARD, D. VERNAT, Acta Materialia vol.58, **2010,** p.3390
[5]G. BERNARD-GRANGER, C. GUIZARD, S. SURBLÉ, G. BALDINOZZI, A. ADDAD, Acta Materialia vol. 56, **2008**, p.4658
[6] JACOBSON, A. J., Chemistry of Materials, vol.22, **2009**, p. 660.